Arabian Journal for Science and Engineering
https://doi.org/10.1007/s13369-024-08717-z

RESEARCH ARTICLE-MECHANICAL ENGINEERING

# Investigation of a Photovoltaic–Thermal Solar Dryer System with Double-Pass Solar Air Collectors and Absorber Surfaces Enhanced with Graphene Nanoparticles

**Murat Öztürk[1,2] · Coşkun Yüksel[1] · Erdem Çiftçi[3]**

Received: 9 October 2023 / Accepted: 31 December 2023


**Abstract**
As a result of increasing energy demand, seeking eco-friendly and sustainable energy resources increases the interest in renewable energy, specifically solar energy. In this study, a novel photovoltaic–thermal solar dryer system with double-pass solar air collectors and nano-enhanced absorber surface was developed, and its performance was experimentally investigated. Initially, a double-pass solar dryer (DPSD) with an absorber surface of flexible aluminum ducts coated with black matte paint was produced. Then, a double-pass solar dryer (NDPSD) consisting of flexible aluminum ducts coated with graphene and black paint was designed. These two systems were experimentally and simultaneously examined, and parameters such as energy and exergy efficiency, drying rate, and moisture ratio, which are the performance indicators of solar air collectors and the drying process, were analyzed. The sustainability parameters were also considered as a part of the analysis. The mean thermal efficiency of the solar air collectors for DPSD and NDPSD was calculated as 57.23 and 73.36%, respectively, where the airflow rates were measured as 0.024 and 0.017 kg/s. Furthermore, under the same airflow rate conditions, while the mean exergy efficiency of the collector was 27.77% for NDPSD, it was calculated as 16.64% for DPSD. Moreover, exergy efficiencies of the drying chamber varied between 27.35% and 82.20% for NDPSD and between 21.03 and 81.25% for DPSD, under the airflow rates of 0.012–0.016 kg/s conditions, respectively.

**Keywords** PVT · Double-pass solar dryer · Graphene · Energy–exergy · Sustainability

## List of symbols

| | |
|---|---|
| A | Area ($m^2$) |
| $c_p$ | Specific heat capacity (kJ/kgK) |
| COP | Coefficient of performance |
| DC | Drying chamber |
| DPSD | Double-pass solar dryer |
| DR | Drying rate |
| $\dot{E}$ | Useful energy rate (W) |
| EF | Experimental finding |
| FF | Fill factor |
| G | Solar radiation ($W/m^2$) |
| $I$ | PV current (A) |
| $I_{sc}$ | Short-circuit current (A) |
| $\dot{m}$ | Air mass flow rate (kg/s) |
| MR | Moisture ratio |
| NDPSD | Nano-enhanced double-pass solar dryer |
| PV | Photovoltaic cell |
| SEC | Specific energy consumption |
| $\dot{Q}$ | Heat transfer rate (W) |
| SI | Sustainability index |
| $U$ | Uncertainty |
| $t$ | Time/min |
| $T$ | Temperature (°C) |
| $v$ | Velocity (m/s) |
| $V$ | PV voltage (V) |
| $V_{oc}$ | Open-circuit voltage (V) |
| $w$ | Water |
| $W_f$ | Energy consumption of fan (W) |
| WER | Waste exergy ratio |
| $X_{in}$ | Exergy inflow (W) |

✉ Erdem Çiftçi
erdemciftci@gazi.edu.tr

[1] Graduate School of Natural and Applied Sciences, Gazi University, Ankara, Türkiye

[2] Department of Mechanical Engineering, National Defence University, Ankara, Türkiye

[3] Department of Energy Systems Engineering, Gazi University, Ankara, Türkiye

Published online: 31 January 2024

| | |
|---|---|
| $X_{\text{loss}}$ | Exergy loss (W) |
| $X_{\text{out}}$ | Exergy outflow (W) |
| $x$ | Independent variable |

## Greek symbols

| | |
|---|---|
| $\alpha$, | Absorptivity |
| $\eta_{th}$ | Thermal efficiency |
| $\eta_X$, | Exergy efficiency |
| $\eta_e$, | Electrical exergy |
| $\rho$, | Density (kg/m$^3$) |
| $\tau$ | Transmittance of the glass cover |

## Subscripts

| | |
|---|---|
| $a$ | Air |
| abs | Absorber surface |
| colc | Collector |
| env | Environment |
| $e$ | Electrical |
| in | Inlet |
| loss | Loss |
| max | Maximum |
| oc | Open circuit |
| sc | Short circuit |
| sun | Sun surface temperature |
| out | Outlet |
| use | Useful |

## 1 Introduction

Energy demand has been rising gradually owing to the growing population worldwide. Increasingly exhausted energy resources are a major problem as well. At this point, concerns about a sustainable future happen. One of the most serious concerns is the need for nourishment. With population growth, an increase in food requirements is also occurring. Therefore, it is vital to store nourishment for use in the future. Apart from these requirements, this storage is highly valued for personal comfort. Similarly, products that are impossible to grow or reach during the seasons may be crucial to store for subsequent usage. Besides, in such cases as long-term travel, it may be possible to move from one point to another without any damage by applying various processes for foods that can deteriorate quickly. In this aspect, one of the most preferred methods is drying the product. Various methods are available for drying, including artificial, combined, freezing, and solar drying. Solar drying is a widely preferred method since these systems are generally easy to build, sustainable, and require no costly maintenance. The traditional drying process with solar energy from the past to the present has occurred by spreading the food outdoors. However, this is an unclean and inefficient method that needs to be transformed into an even more advanced form. At this point, different studies have been carried out on solar drying systems. Kong et al. [1] studied the characteristics of a new drying system compared to traditional drying systems. Their developed dryer unit included a photovoltaic–thermal solar air collector with a monocrystal photovoltaic system, and they selected turnips as a drying product. Their results provided that the solar dryer system dried less than the traditional natural drying time, and the humidity level with the solar dryer declined from 20.370 to 0.197. In contrast, the humidity level with traditional natural methods reduced from 21.320 to 0.250 and took longer. Besides, the product was reported to have mold due to traditional drying. Ortiz-Rodriguez et al. [2] studied two rubber plate drying systems. In this study, they carried out a performance analysis of direct and indirect solar-powered drying systems. As a result of their study, it was declared that the drying process lasted 12 days in the direct system and nine days for an indirect system, and the solar air collector efficiency was 33.77%. They reported that the direct system was recommended for small operations, while the indirect system was more appropriate for large industrial processes. Gurel et al. [3] performed an experimental and numerical study to examine a fluidized bed-type solar drying system, which was temperature controlled. In this study, they designed a fluidized bed-type solar drying system that includes flat plates or zigzag blades. As a result of their observations, the overall system efficiency was 64%. Besides, the exergy efficiency was reported as 7.2% for flat plate systems and 11.6% for zigzag plate systems. A solar dryer tunnel to remove moisture from the sewer mud was designed and studied by Afshari et al. [4]. They examined three types of models: rectangular, quonset, and finned quonset with CFD modeling to determine the most appropriate model at first and then experimentally investigated the Quonset type solar tunnel due to these procedures. The results found that the fins improved the performance of the Quonset model by 17.2%, and Quonset dryers were reported to operate well. Sözen et al. [5] designed an indirect solar dryer system including a tube-shaped absorber surface and analyzed its performance. They also integrated aluminum wool material to upgrade the absorber tubes' thermal efficiency. The success of tube-absorbing surfaces developed due to experimental and numerical analysis has been emphasized; with aluminum wool insertion, a 30% reduction in drying time was reported. Sözen et al. [6] conducted a numerical and experimental study to assess the alterations in thermal performance by adding the iron mesh to the indirect solar dryer with a tube absorber. In this study, they examined two types

of models: hollow pipe heater and iron mesh-modified heater. As a result, it is stated that using iron mesh increases thermal efficiency by up to 11%. Tuncer et al. [7] investigated the performance of a greenhouse dryer they designed by integrating it with a new solar air collector for performance improvement. In this study, they integrated a solar air collector with four-pass into the greenhouse-type dryer, and they investigated the drying process of the red pepper–kiwi products. They stated the designed system's thermal efficiency altered between 71.63 and 80.66%. Moreover, the specific moisture extraction rate of 0.21–0.36 kg/kWh was calculated for red pepper and kiwi products, respectively. Şevik et al. [8] studied a system where the mint and apple slices were dried via solar energy. In this study, they designed two dual-pass solar air dryer systems with and without infrared support, and the performance of each system was examined. In the outcomes, integrating infrared into the system notably increased energy consumption, and the infrared lamp protected the products from deterioration. It was also stated that the developed system had high dehumidification performance. Krabch et al. [9] investigated a drying system utilized for orange drying in a region in Morocco. In this study, they developed three types of dryer models. The first model consisted of a solar air collector and a drying unit. In contrast, the second version included a drying room and a double-glazed absorbent surface, and the third model included a single surface of absorbent material. Their obtained data showed that the time taken to lose 72% of the mass of the dried orange slices was reported to be six days in the third system, 18 days in the second system, and 15 in the first system. Hassan et al. [10] studied a V-grooved type dual-pass solar-powered dryer for performance evaluation. In this study carried out in an area in Australia, the apple product was dried, and calculated data indicated that the maximum thermal efficiency is 88.8% and exergy efficiency is 6.6%. Veeramanipriya and Sundari [11] designed a new photovoltaic–thermal system to dry cassava in Indian conditions. The researchers used A hybrid photovoltaic–thermal system containing a vacuum tube solar collector. They indicated that the dried product significantly reduced humidity in 8 h. Kale and Havaldar [12] conducted a review study to determine the techniques required to provide a performance increment in indirect solar dryers. They stated that phase exchange materials were indicated to be very interesting due to thermal energy storage capability to provide improvement in overall system performance. It is also stated that the performance can be increased by integrating the photovoltaic panel into the indirect-type dryers. Gilago et al. [13] experimentally analyzed the two solar dryers that were integrated with and without an energy storage unit. They utilized paraffin as thermal energy storage media. Their results indicated the efficiency values of the energy storage-integrated system were reported to be more effective than the other system.

On the other hand, different variations have also been implemented to improve the performance of such systems, like coating the absorber surface with nanoparticles. To illustrate, Al-Kayiem et al. [14] investigated nanomaterials' effects on solar air heaters' performance. This work tested five types of absorbent surfaces painted with standard: dolphin black paint, $Al_2O_3$ nanoparticles-added black paint, CuO-coated paint, and finally, black paint with an $Al_2O_3$-CuO mixture. Their outcomes denoted that the insertion of nanoparticles into the dye increased the system efficiency remarkably. Nazari et al. [15] conducted a study to investigate the influence of nanoparticles on the absorbent surface and overall system performance. They coated the absorber surfaces of the solar heater with CuO nanoparticles. They analyzed the performance of 3 varying species of absorber plates (copper plate, black-painted plate, and CuO-coated plate). As a result, the nanoparticles-included system was reported to provide a performance improvement of 18.8% compared to the black dye-coated system and 35.8% compared to the standard copper. Selimefendigil and Şirin [16] studied experimentally the performance of three various photovoltaic–thermal systems, that is, traditional photovoltaic–thermal system (PVT), PVT with paraffin-included thermal energy storage, PVT with CuO nanoparticles, and paraffin-included thermal energy storage. According to their results, the use of nanoparticles can be accompanied by a significant increase in performance. To enhance the performance of the greenhouse dryer, Selimefendigil et al. [17] integrated the north wall coated by graphene-doped black dye into the greenhouse dryer and compared the standard north wall to the integrated type of greenhouse dryer. The results provided that the nanoparticle addition process nearly doubled the system's exergy efficiency.

Another significant point was that drying time was reduced by adding the nano-coated north wall to the standard system. Sivakumar et al. [18] studied the impact of flat-plate absorber surfaces covered with CuO nanoparticles on drying performance. In this study, realized in India, they examined two systems: an absorber surface coated with traditional black paint and an absorber surface with different fractions of CuO. According to their findings, where the highest temperature was achieved, the system increased the collector efficiency by 4% and decreased the drying time by 6%. Selimefendigil et al. [19] studied the impact of nano-coating on the absorber surface of the solar heater that supports the greenhouse drying system. Using the three-pass flow system, they coated the absorber plate with CuO nanoparticles and experimentally analyzed it. Their main observation was that the nano-coated system significantly decreased the drying time. Khanlari et al. [20] examined the performance of a newly designed vertical solar air heater with nano-coating and perforated baffles. In this study, they performed system performance analysis by applying standard

matte black dye and CuO-inserted black dye to the absorber of solar collectors. They found that the thermal efficiency of the nanoparticle-included system varied between 58.10 and 76.22%, while the standard system had a thermal efficiency of between 54.96 and 72.05%. Besides, it was emphasized that with the addition of nanoparticles into the dye, the exergy efficiency was increased. Abdelkader et al. [21] examined nanoparticles' influence on solar air heaters' performance. In their study, they sprayed mixing carbon nanotubes and CuO nanoparticles with different levels of black paint from 0 to 5% and then sprayed them into flat-plate absorber surfaces. Their results indicated that the system with 4% CNTs/CuO-black dye reached the maximum solar absorption value at 90.16% and was more efficient than others. Kabeel et al. [22] aimed to increase system efficiency by applying $TiO_2$ nanoparticles mixed with black dye to the absorbent surface of the triangle pyramid solar purifier. They examined the performance of this system at depths of water between 1 and 3.5 cm. The results of the experiments showed that the usage of nanoparticles upgraded the water temperature in proportion to the increase in water depth. Daily freshwater production was also reported to have improved by around 6% by integrating these nanoparticles. Kumar et al. [23] focused on increasing the performance of the triangle solar air heater. Herein, they covered the absorber surface of the solar air heater with 1.0% graphene embedded in the black paint. This experimental study studied the parameters linked to the glass temperature and the absorber plate. The remarkable point of their research is that the graphene-coated system had a higher efficiency value than the system with no coating.

The cost is also one of the most critical parameters during the design process of a drying system. Hence, it is aimed at achieving maximum efficiency at the optimum prices. Different types of absorber surfaces and collectors have been designed from various materials, and many researchers have investigated their performance. Güler et al. [24] developed a low-cost solar dryer. In this study, they compared the double-pass indirect solar dryer to the double-pass indirect solar dryer absorber, which was modified. They chose Pepino fruit for the drying process in this study. They indicated that they obtained the best drying efficiency from the mesh absorber system at the rate of 23.08%. Khanlari et al. [25] investigated the performance upgrading of the greenhouse dryer under cost-effective conditions. In this study, they integrated a tube-type solar heater into the greenhouse dryer. They selected the apricot as a drying product in this system, which is experimentally and numerically examined and operated under different conditions. The data showed a significant decline in drying time with the integrated system. Krabch et al. [26] designed a single-pass indirect solar dryer at the point of developing food drying systems. They used the pears for drying products and declared that meager humidity rates were obtained along with the designed system. Gill et al. [27] experimentally analyzed the performance of a cost-effective solar air heater. They used materials that would require a low cost, such as thermocol, ultraviolet-stabilized plastic sheets, etc. The tests and calculations indicated that the designed system may be used for small-scale drying due to their appropriate costs. Poole et al. [28] studied a low-cost solar air heater to grow a turkey. In this study, the transpired solar collector made of the black plastic plate was investigated and produced cheaply. The developed system was reported to be appropriate for agricultural, commercial, and industrial use. Ahmad [29] studied a low-cost solar air collector from plastic packaging films. This drying system initially used a single-layer cylindrical structure and was then modified with an air bubble plastic coating. This efficient system was indicated to minimize heat transfer of an air bubble plastic coating. Ndukwu et al. [30] developed a low-cost drying system. They examined the active mix-mode wind-powered fan solar dryer and passive mix-mode non-wind-powered solar dryer in their design. They used glycerol as a thermal storage material and experimentally investigated the dryer's performance. Their findings showed that the active mix-mode wind-powered fan solar dryer with integrated glycerol took less time to dry than others.

A new solar dryer was produced and tested experimentally in this experimental study. The energy and exergy analysis was performed not only for solar collectors but also for the drying chamber. The sustainability indicators were also calculated. Absorber surfaces, which initially consisted of flexible aluminum ducts, were coated with black matte paint. A new solar dryer with an absorber surface of aluminum flexible ducts covered with black matte paint mixed with graphene was designed. The systems were developed as double-pass, and the performance of each was examined simultaneously. As a drying product, carrot slices were utilized. In this study, a tube-type absorber surface, which is also enhanced by graphene nanoplatelet, compared to conventional plate counterparts, was used to improve the performance of a solar air collector system. Besides, the obtained hot air was used to dry a product. This work also highlighted the investigation of electrical performance in terms of the second law of thermodynamics. The main aim of this work is to show off the utilization of a renewable energy resource for industrial processes and specify the environmental effects considering the sustainability index parameter. Figure 1 shows the steps followed in this experimental investigation.

## 2 Material and Method

### 2.1 Details of the PVT System

In this work, two newly developed photovoltaic–thermal solar air dryer systems were fabricated, and the performance

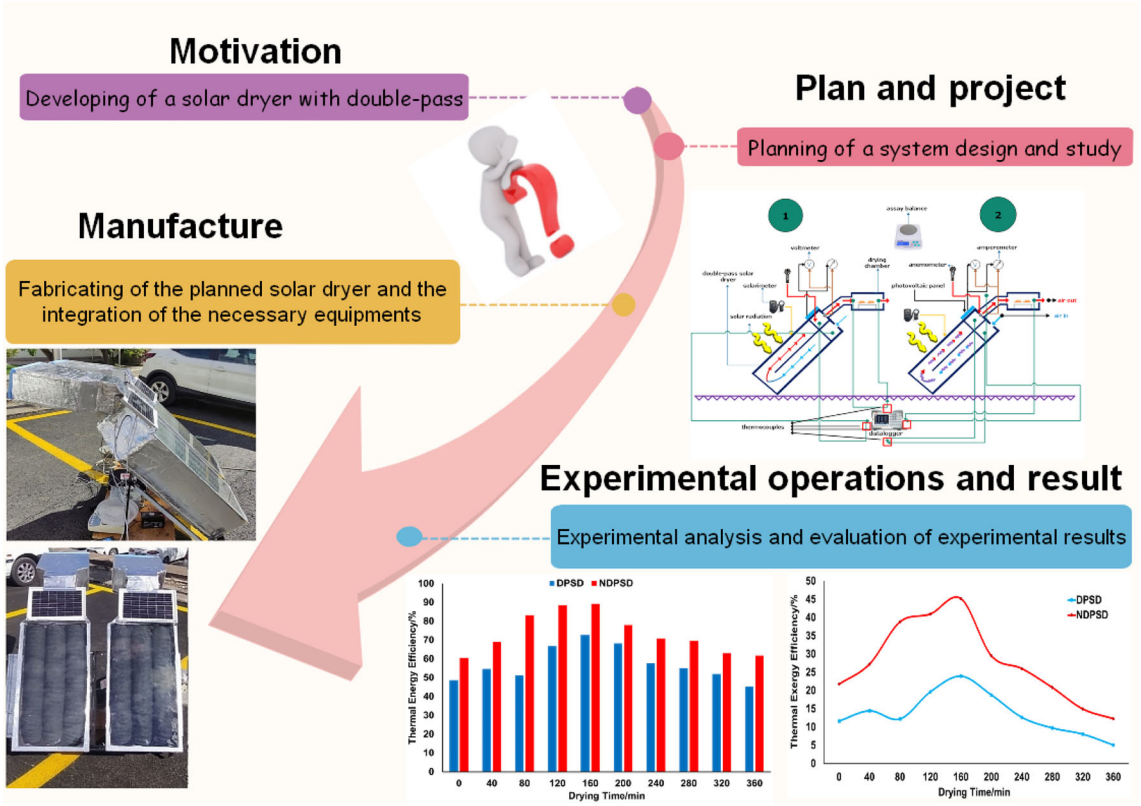


**Fig. 1** Main steps followed during the study

of each system was investigated by considering various parameters. The study utilized a double-pass solar air collector with two different absorber plates. The absorber plates of one of the designed collectors were painted with standard black matte paint, and the other one was covered with black matte paint mixed with graphene nanoparticles. There are many reasons why graphene nanoparticles were preferred. Graphene, also known as the honeycomb structure of carbon, has a fine structure, very high surface area, and thermal conductivity. For instance, for monolayer graphene, the surface area and thermal conductivity at room temperature are 2630 $m^2/g$ and 5000 W/mK, respectively [31]. The utilized graphene nanomaterial was purchased from *Nanografi Nanotechnology Company* as milled powders and is in nanoplatelet form. It has a 5 nm thickness and a diameter of 30 μm. Besides, the specific surface area is 1700 $m^2/g$.

Unlike conventional solar air collectors, flexible aluminum ducts were used instead of absorber plates in a flat rectangular shape. The aim is to provide a more extended interaction between solar energy and air, thus increasing the air exit temperature. Besides, the fact that the utilized materials are more affordable in terms of price is another advantage of the designed systems.

The collector case and solar air dryers' drying chamber sections were built using Styrofoam insulation. The collector case and the drying chamber were covered with aluminum tape to protect against sunlight in the outdoor environment. Except for the area where the absorber plates are located, all external parts of the experimental setup were similarly covered with aluminum tape to protect them from the adverse influences of solar radiation and to maintain insulation for the system. After the experimental setup was built, the tests were implemented on both systems simultaneously, and the results were analyzed comparatively. A schematic of the designed systems is depicted in Fig. 2. The dimensions of the experimental setup are also given in Fig. 3.

As illustrated in Fig. 2, K-type, eight thermocouples were employed to take temperature measurements of the specific locations. Each thermocouple was connected to the datalogger, and the measurements were recorded. An assay balance was utilized to examine the variations in product weights during drying. Furthermore, a solarimeter and an anemometer were used to measure solar irradiation and air flow rate, respectively. A multimeter measured the voltage and current values of the electrical energy produced in the photovoltaic panel at regular intervals. The other specifications of the device/equipment employed in the measurements are presented in Table 1. The electrical energy requirement of the

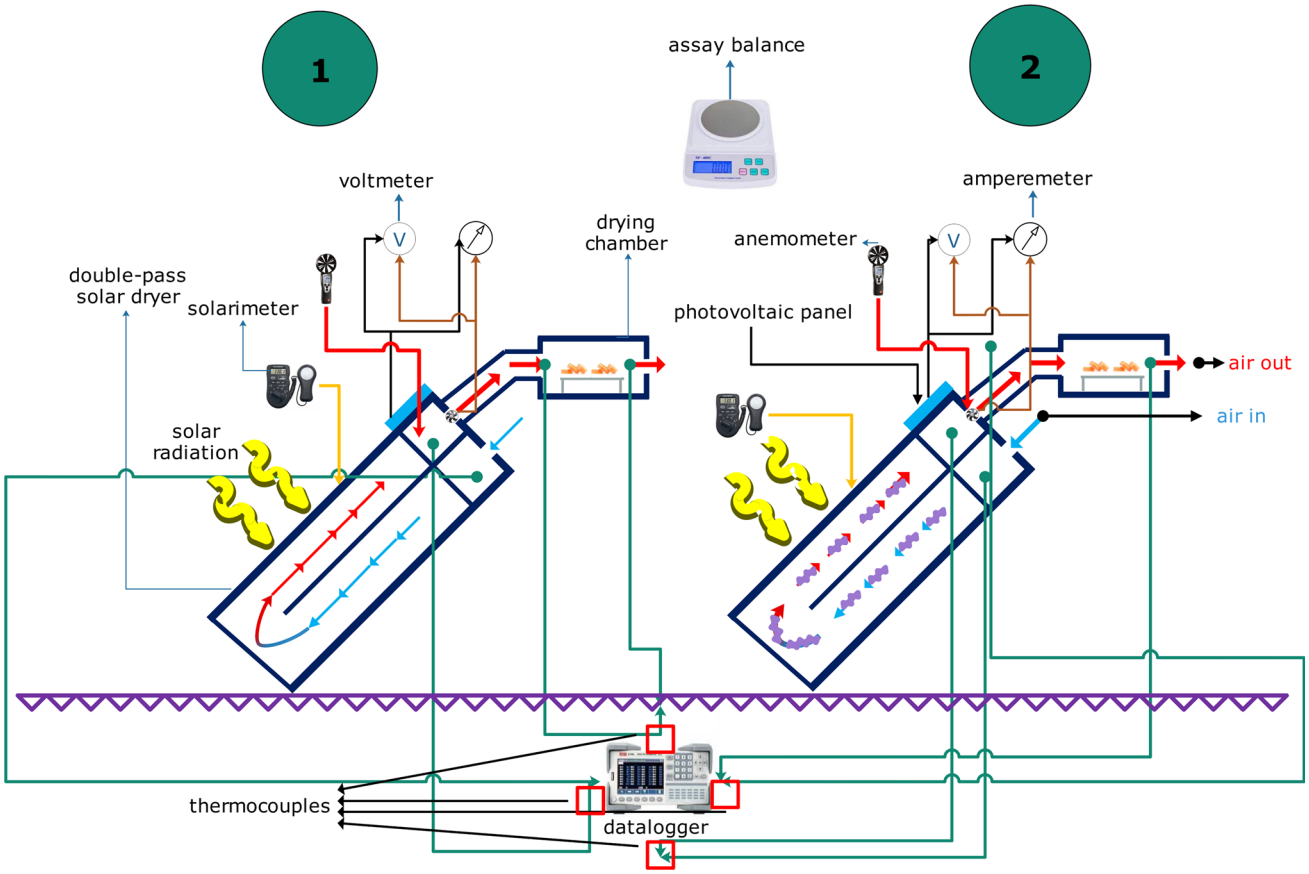


**Fig. 2** Schematic of designed solar dryers: (1) DPSD and (2) NDPSD

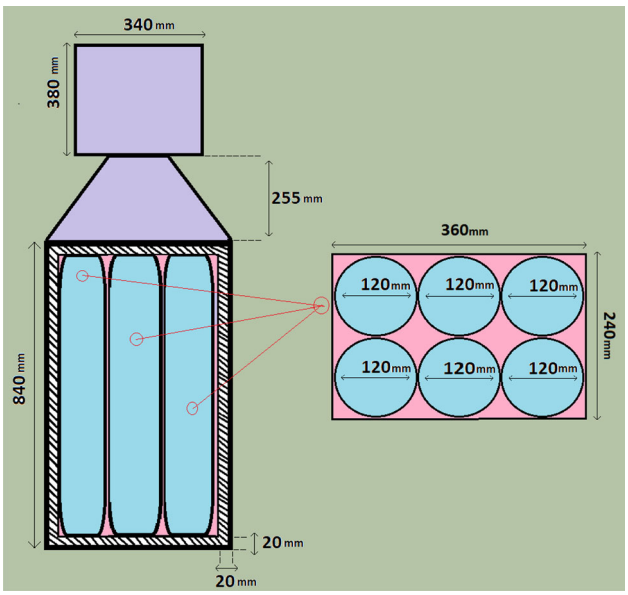


**Fig. 3** Dimensions of the solar collector and drying chamber

fans in the system was provided by photovoltaic panels, details of which are provided in Table 2, integrated into each collector case. Each photovoltaic panel was initially

**Table 1** Some details of the measurement equipment/devices

| Equipment/device | Range | Accuracy |
|---|---|---|
| Datalogger | −40 + 1760 °C | ± % 0.5 °C |
| Thermocouples | −200 + 1200 °C | ± % 0.5 °C |
| Solarimeter | 0–1300 W/m$^2$ | ± % 0.5 W/m$^2$ |
| Anemometer | 1.00–30.00 m/s | ± %3 m/s |
| Assay balance | 0–6000 g | ± 0.01 g |
| Multimeter | 1000 V/10 A | ± 0.8%/ ± 2% A |

**Table 2** Specifications of PV panels employed in the system

| Parameter | Specifications |
|---|---|
| Model | Solarinka solar panel |
| Maximum power ($P_{max}$) | 12 W |
| Maximum voltage ($V_{max}$) | 23.25 V |
| Maximum current ($I_{max}$) | 0.52 A |
| Open-circuit voltage ($V_{oc}$) | 23.45 V |
| Short-circuit current ($I_{sc}$) | 0.58 A |
| Size | 355 × 255 × 20 mm |

**Fig. 4** Prepared carrot samples for drying and the utilized perforated tray

connected to the battery, and thus, it is aimed to provide uninterrupted power to the fans in the system.

### 2.2 Details of the Drying Process

The experiments were carried out at Gazi University, Ankara, Turkey. The solar collector of each drying system was placed on platforms inclined 40° and positioned in the south direction in order to absorb maximum solar radiation from the sun, based on the yearly average daily solar radiation values for Ankara province [32]. The experiments were run between 10:00 AM and 4:00 PM. Fans of 70 × 70 mm provide air suction with 40 W power, and the resulting hot air is oriented to the drying chamber. The process of drying carrot slices was carried out in the drying chamber. For this purpose, two samples, each 50 g, were prepared (Fig. 4). Perforated trays were preferred for drying; thus, hot air contact was ensured to the dried product from the upper and lower surfaces. The weights of the collected samples were recorded every 40 min through assay balance. Similarly, the current and voltage values of the photovoltaic panels and fans were measured and recorded every 40 min. In addition, the collector air inlet temperatures and the drying chamber air inlet and exit temperatures were recorded simultaneously every 40 min. Figure 5 illustrates the test rig with different aspects.

## 3 Theoretical Analysis

This section of the paper presents the formulas used in the performance analysis of the designed solar dryers. The theoretical equations for calculating solar collector, PV panel, and drying process were discussed in separate subsections.


**Fig. 5** (**a**) Front, (**b**) back, and (**c**) side views of the designed test rig

### 3.1 Calculation of Solar Collector-Related Parameters

Considering the general form, the conservation of energy for solar collectors can be calculated by Eq. (1) and Eq. (2) [20]:

$$\dot{E}_{in} = \dot{E}_{out} \tag{1}$$

$$\dot{E}_{in} = \dot{E}_{use} + \dot{E}_{loss} \tag{2}$$

Similarly, the conservation of mass is:

$$\dot{m}_{in} = \dot{m}_{out} \tag{3}$$

where the mass flow rate of each system can be computed as follows:

$$\dot{m} = \rho \mathrm{v} A_{colc} \tag{4}$$

As a result of the obtained data, the energy input of the designed collector is calculated by Eq. (5) [20]:

$$E_{in_{colc}} = \tau \alpha G A_{colc} \tag{5}$$

The amount of useful energy in each collector must be calculated to find the collector's performance as a result of calculating the power provided by the solar energy. Based on

the temperature difference, it can be determined via Eq. (6) [20]:

$$\dot{E}_{use_{colc}} = \dot{m}_a c_p (T_{out} - T_{in}) \tag{6}$$

Thereby, the efficiency of the solar collector is [20]

$$\eta_{th_{colc}} = \frac{\dot{E}_{use_{colc}}}{\dot{E}_{in_{colc}}} = \frac{\dot{m}_a c_p (T_{out} - T_{in})}{\tau \alpha I A_{colc}} \tag{7}$$

The exergy of the system is one of the fundamental parameters to be considered in solar air collectors. In this aspect, the exergy efficiency can be calculated by the following formula [20]:

$$\eta_{X_{colc}} = \frac{X_{out_{colc}}}{X_{in colc}} \tag{8}$$

where the exergy inflow of the solar collector is [20]:

$$X_{in}olc = X_{loss_{colc}} + X_{out\,colc} \tag{9}$$

Each term in Eq. (9) can be calculated as follows [20]:

$$X_{incolc} = \left(1 - \frac{T_{env}}{T_{sun}}\right) G \tag{10}$$

$$X_{outcolc} = \dot{m}_a c_p \left[ (T_{out} - T_{in}) - T_{env} \ln\left(\frac{T_{out}}{T_{in}}\right) \right] \tag{11}$$

$$X_{losscolc} = \left[ \left(1 - \frac{T_{env}}{T_{sun}}\right) G \right] - \dot{m}_a c_p \left[ (T_{out} - T_{in}) - T_{env} \ln\left(\frac{T_{out}}{T_{in}}\right) \right] \tag{12}$$

The coefficient of performance (COP) of the collector is [20]

$$COP = \frac{\dot{E}_{use_{colc}}}{W_f} \tag{13}$$

where $\dot{E}_{use_{colc}}$ and $W_f$ are the useful energy provided by the collector and the fan's energy consumption, respectively.

### 3.2 Calculation of Photovoltaic Panel-Related Parameters

The PV panel's electrical energy and exergy efficiency can be calculated by Eqs. (14) and (15), respectively [20].

$$\eta_e = \frac{E_{e_{PV}}}{E_{in}} \tag{14}$$

$$\eta_{X_e} = \frac{X_e}{X_{in}} \tag{15}$$

where the electrical power of the PV panel is calculated as follows [20]:

$$E_{e_{PV}} = X_e = V_{oc} I_{sc} FF \tag{16}$$

Similarly, energy input and exergy inflow into each PV panel is [20]

$$E_{in} = \tau \alpha G A_{PV} \tag{17}$$

$$X_{in} = \left(1 - \frac{T_{env}}{T_{sun}}\right) G \tag{18}$$

The fill factor (FF) is [20]

$$FF = \frac{I_{max} x V_{max}}{I_{sc} x V_{oc}} \tag{19}$$

### 3.3 Calculation of Drying Parameters

Considering the general form of conservation of energy and conservation of mass formulas, the following equations can be expressed for the drying chamber [24, 25]:

$$\dot{m}_{in_{DC}} = \dot{m}_{out_{DC}} \tag{20}$$

$$\dot{E}_{in_{DC}} = \dot{E}_{out_{DC}} \tag{21}$$

As far as the energy equation (Eq. 22) is concerned, a detailed formula can be written as follows [24, 25]:

$$\dot{Q}_{net} + \sum \dot{m}_{DC} \left( h_{in_{DC}} + \frac{v^2_{in_{DC}}}{2} + z_{in} g \right) = \sum \dot{m}_{DC} \left( h_{out_{DC}} + \frac{v^2_{out_{DC}}}{2} + z_{out} g \right) + W_{net} \tag{22}$$

As a result of these findings, specific energy consumption (SEC) can be calculated, which is the ratio of the amount of moisture withdrawn from the products in the drying chamber to the electrical energy consumed in the solar air dryer [24, 25].

$$SEC = \frac{E_{in}}{m_w} \tag{23}$$

Another prominent parameter for drying processes is the moisture ratio (MR) of the product, which is calculated by

Eq. (24) [24, 25]:

$$MR = \frac{m_i - m_f}{m_f} \tag{24}$$

Similarly, the drying rate is [25]

$$DR = \frac{MC_{t+\Delta t} - MC_t}{\Delta t} \tag{25}$$

where "$t$" and related expressions represent the parameters that change depending on time.

Exergy inflow of the drying chamber is [25]

$$X_{in\,DC} = X_{loss\,DC} + X_{out\,DC} \tag{26}$$

where

$$X_{in\,DC} = m_{DC} c_{p_{air}} \left[ \left( T_{in_{DC}} - T_{env} \right) - T_{env} \ln \left( \frac{T_{in_{DC}}}{T_{env}} \right) \right] \tag{27}$$

$$X_{out\,DC} = m_{Dc} c_{p_{air}} \left[ \left( T_{out_{DC}} - T_{env} \right) - T_{env} \ln \left( \frac{T_{out_{DC}}}{T_{env}} \right) \right] \tag{28}$$

Accordingly, the exergy efficiency of the drying chamber can be calculated as follows [24, 25]:

$$\eta_{X_{DC}} = \frac{X_{out\,DC}}{X_{in\,DC}} \tag{29}$$

Finally, for the illustration of the sustainability level of the designed system, the sustainability index (SI) and coefficient of performance (COP) values can be computed using Eqs. (30) and (31), respectively [24, 25]:

$$SI = \frac{1}{1 - \eta_{X_{DC}}} \tag{30}$$

$$COP = \frac{E_{use_{DC}}}{W_f} \tag{31}$$

### 3.4 Uncertainty Analysis

Determination of the uncertainties in experimental work is crucial in terms of the accuracy of the obtained results. Considering the uncertainty calculation approach suggested by Holman [33], the uncertainties of the experimental devices or instrumentations were calculated. Equation (32) presents the mathematical formula utilized for the calculations:

$$U_{EF} = \left[ \left( \frac{\partial F}{\partial x_1} u_1 \right)^2 + \left( \frac{\partial F}{\partial x_2} u_2 \right)^2 + \left( \frac{\partial F}{\partial x_3} u_3 \right)^2 \ldots + \left( \frac{\partial F}{\partial x_n} u_n \right)^2 \right]^{1/2} \tag{32}$$

**Table 3** Uncertainty analysis results

| Instrument type | Technical specifications | Accuracy | Uncertainty |
|---|---|---|---|
| Datalogger | −40 + 1760 °C | ± 0.5% | ± 0.6728 |
| Thermocouples | −200 + 1200 °C | ± 0.5% | ± 1.1180% |
| Assay balance | 0–6100 g | ± 0.01 | ± 1.0000% |
| Solarimeter | 0–1300 W/m$^2$ | ± 0.5% | ± 1.1456% |
| Anemometer | 1–30 m/s | ± 3% | ± 1.1192% |

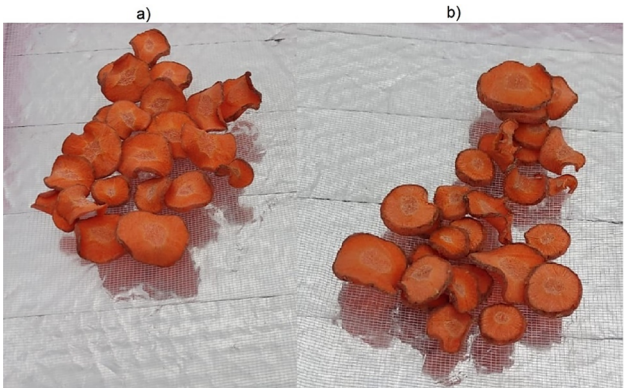


**Fig. 6** Photographs of the samples after the drying process in (**a**) DPSD and (**b**) NDPSD system

where $U$ denotes the uncertainty; $EF$, $x$, and $u$ represent the measured experimental result, the independent variable, and the uncertainty of the independent variable, respectively. The errors resulting from data reading from the instruments and the junctions, and based on the equation above, the uncertainty in this work ranged around ± 1% (Table 3).

## 4 Results and Discussion

The obtained findings based on the experiments were processed and discussed with the related theoretical formulas in this part of the paper. Varying illustrations were employed to understand the findings better.

Figure 6 displays the final condition of the samples after the drying process in the solar dryers designed. When both photographs were examined, it was seen that the drying rate of the sample dried in the system with the absorber plate painted with nanoparticle-added paint was higher compared to the other system. Moreover, it can be said that the effective heat transfer area, which increases with the double-pass design and the utilization of aluminum ducts, significantly reduces the drying time of the product.

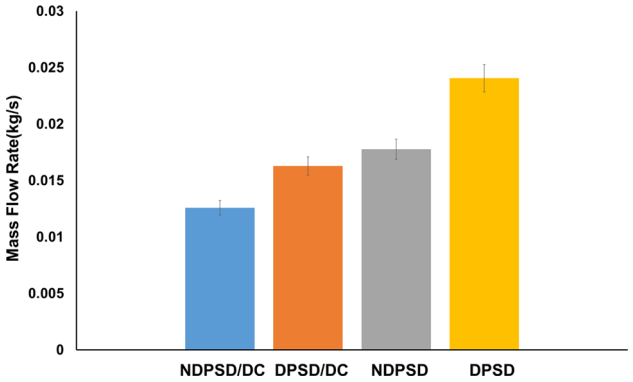


**Fig. 7** Airflow rates measured at the dryer and solar collector

As stated earlier, the tests were performed under varying air flow rates to address how flow rate influences the changes in air temperature and drying parameters. Figure 7 presents the measured air flow rates in the drying chamber and the collector. While the mean air flow rate of the nano-coated system in the solar collector was 0.017 kg/s, the mean air flow rate of the system covered with black matte paint was 0.024 kg/s. The average air flow rate, in addition, in the drying chamber of the system with an absorber surface painted with nanoparticle-added paint was measured as 0.012 kg/s, while the average air flow rate in the drying chamber of the system covered with black matte paint was measured as 0.016 kg/s.

Figure 8 displays the alteration in environment temperatures during the experiment. The mean value of the temperatures measured during the day was calculated as 28.21 °C. Besides, the maximum temperature reached during the day was 30.4 °C, while the minimum was 21.6 °C. The designed dryers were analyzed under the same environmental conditions on the same day. Figure 9 shows the solar irradiation changes falling on the dryer systems during the experiments. As stated before, the solar irradiation falling over the collector during the day was measured with a solarimeter. Depending on the data achieved, the average solar irradiation is 953.5 W/m$^2$K. Furthermore, the maximum and minimum solar irradiation was 1270 and 630 W/m$^2$K, respectively. Considering the acquired data regarding the accuracy and reliability of the results, it is possible to state that the weather conditions are pretty favorable for the accurate analysis of the designed systems.

Figure 10 provides the temperature variation at the collector exit of solar dryers whose absorber surfaces were coated with both nano-enhanced and standard black paint. The remarkable point here is that the system, which was painted with black dye with the addition of graphene nanoparticles, reached higher temperatures. Painting the absorber surface with nanoparticle-added paints on solar dryers significantly affected the temperature values and, thus, the air inlet temperature of the drying chamber. This outcome has also been reported in similar studies by other researchers [17–23].

Improving the heat transfer rate of the system at remarkable levels also results in significant enhancements in performance. As can be observed in Fig. 10, the mean collector exit temperature of the solar dryer system with the absorber surface covered with black matte paint was 34 °C. In contrast, the average collector exit temperature of the solar dryer system with the absorber surface covered with graphene-doped black matte paint was 38.29 °C. There is a significant difference between the two systems. Similarly, the average temperature difference of the nano-enhanced system (NDPSD) was reported as 10.8 °C, while the average temperature difference of the system covered with black matte paint (DPSD) was 5.79 °C. This observation indicates that the nanoparticles notably affect the heat transfer rates. When comparing our results with similar literature, Khanlari et al. [34] obtained the mean exit temperature difference of a PV-driven quadruple-flow solar air heater between 13.3 and 23.4 °C. Similarly, Abbas et al. [35] reported that the variation between the collector inlet and exit temperatures of a flat-plate solar air heater according to the single-glass double-glazed structure shows a characteristic ranging from 9 to 27 °C. Consequently, coating absorber surfaces with nanoparticles can be considered one of the applications to obtain a higher temperature increment in solar air collectors.

Nano-coatings significantly improve the transfer rate of solar irradiation collected on the absorber surface to the air circulating in the system. From this point of view, the thermal performance obtained from the nano-enhanced system is expected to be better than the system covered with black matte paint. Figure 11, based on the calculations and measured data, also confirms this observation. The air temperature and solar irradiation rate are also the other parameters on which thermal efficiency depends. With an increment in solar irradiation rate, an increase in thermal efficiency is also observed. Mean thermal efficiency values for NDPSD and DPSD systems were calculated as 73.36 and 57.23%, respectively. The results provided emphasize the significance of nano-coating the absorber surfaces of solar collectors in a solar drying system.

Regarding the thermal efficiency of similar systems, Selimefendigil et al. [19] investigated the triple-pass solar air collectors with and without coatings. They obtained the thermal efficiency of the nano-enhanced system as 75.11%. Similarly, Omojaro and Aldabbagh [36] reported that the maximum thermal efficiency of the double-pass solar air heater with a steel sweat mesh absorber surface was 63.74%.

The exergy of the drying systems is an important parameter as it indicates the availability rate of the energy obtained in the system, and it is anticipated that the exergy has the same trend as the thermal efficiency; that is, both show a

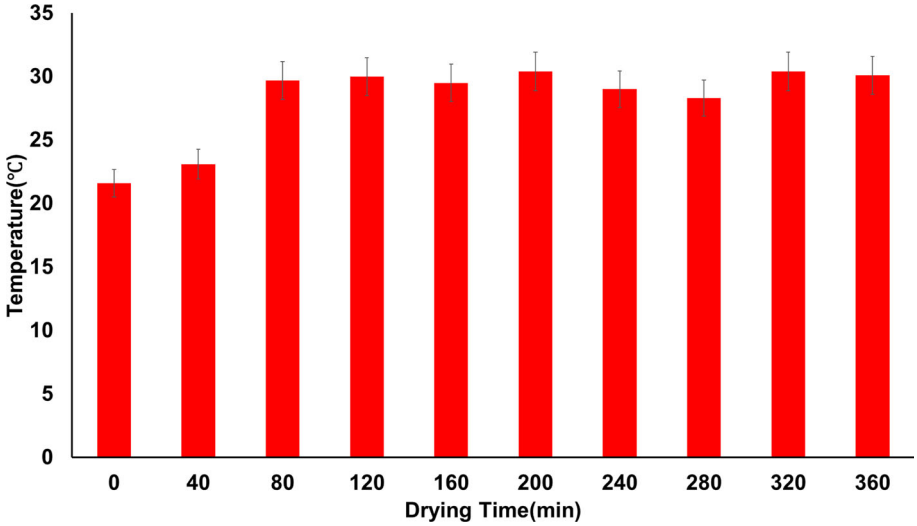


**Fig. 8** Variation in outdoor temperature under different times of the drying process

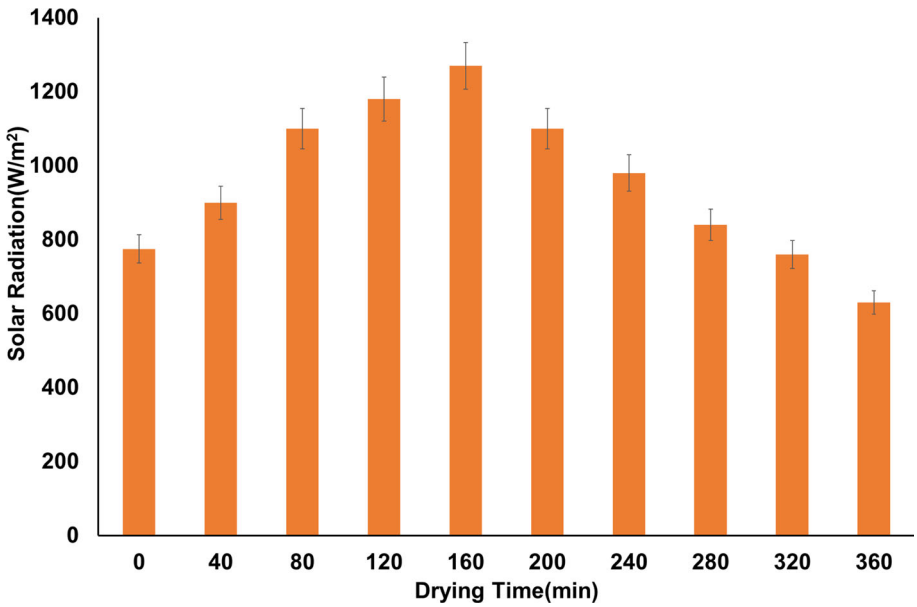


**Fig. 9** Solar irradiation values during the experiments

similar characteristic. In this respect, it is thought that the nano-enhanced system will have a higher exergy efficiency. Figure 12 illustrates the exergy efficiencies of the solar air collectors in the designed solar dryer systems. The mean exergy efficiencies for the designed DPSD and NDPSD systems were calculated as 16.64 and 27.77%, respectively. Since the exergy inflow of the solar collector is approximately constant during the tests, the exergy outflow is more effective on exergy efficiency values. At the beginning of the experiment, the temperature difference between the inlet and exit points of the solar collector is higher. However, as the experiment continues, this difference begins to decline after the thermal equilibrium is provided, which causes exergy outflow to decrease and, thereby, a decline in exergy efficiency. Because the nano-coating increased the heat transfer rate, the exergy efficiency values became higher than those of plain solar collectors. It was observed that similar improvement rates were acquired when the relevant findings were compared with the outcomes of other investigators. Khanlari et al. [20] studied the performance of the vertical solar dryer at different flow rates. They stated that the exergy efficiency of the collectors employed in their system ranged from 11.99 to 14.46%. Abdelkader et al. [21] examined solar air collectors with absorbent surfaces coated with different nanoparticles and obtained system exergy efficiencies between 21.45 and 28.72%.

The exergy efficiencies of the drying chambers of the designed solar dryer systems are presented in Fig. 13. Considering the values in this illustration, the exergy efficiency of the drying chamber of the nano-enhanced system varies between 27.35 and 82.20%. On the contrary, the exergy efficiency of the drying chamber of the system, which has a solar

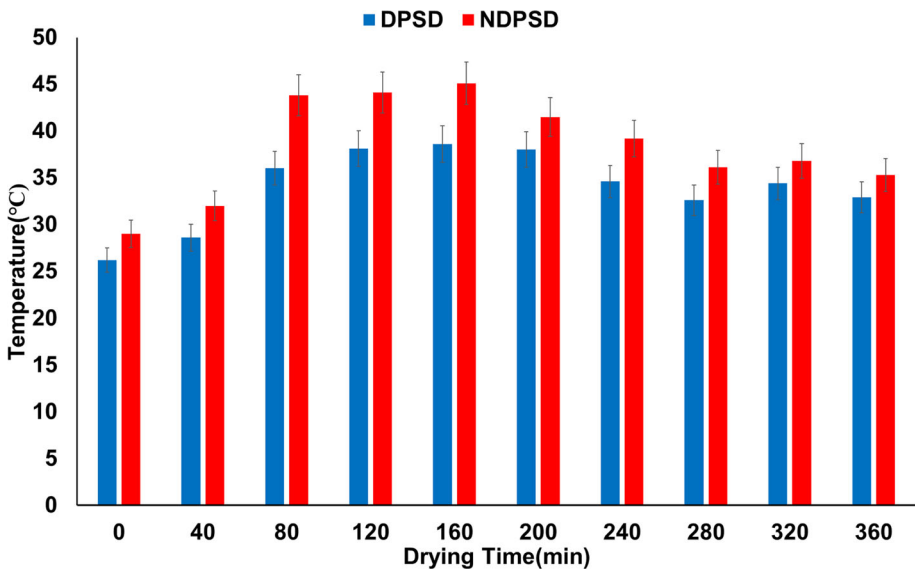


**Fig. 10** Variation in air temperature measured at exit points of the solar collectors

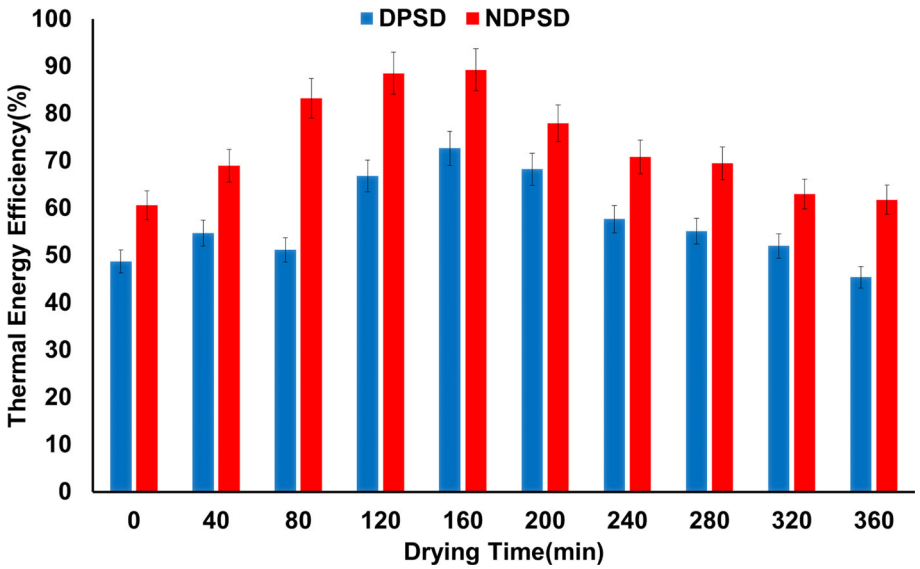


**Fig. 11** Variation in thermal energy efficiency values for solar air collectors

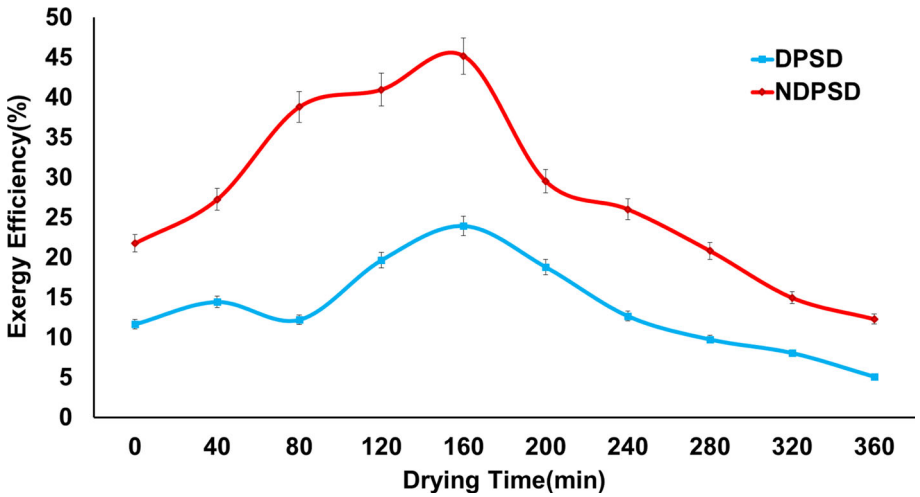


**Fig. 12** Variation in exergy efficiency values for solar air collectors

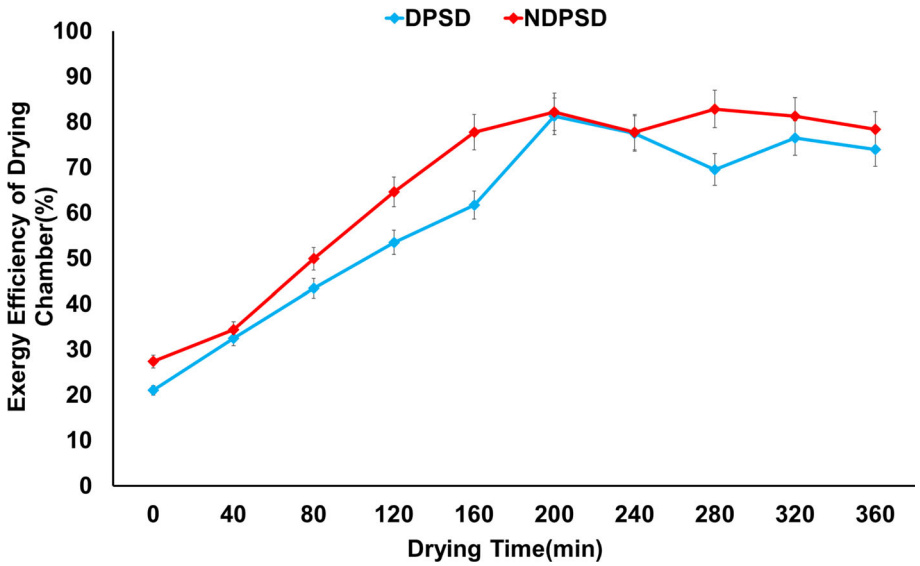


**Fig. 13** Variation in exergy efficiency for drying chambers of each system

collector whose absorber surfaces were painted with standard matte black paint, was calculated between 21.03 and 81.25%. The exergy efficiency of the drying chamber of each system is closely related to the change in the moisture content of the product. It can be said that the exergy efficiency of the drying chamber tends to increase as the humidity decreases. Besides, the system air temperature and environment temperature also affected this condition. System performance is significantly affected by the difference between the environment and drying chamber temperatures. As this difference decreases, an increase in system performance is observed. The exergy efficiency of the drying chamber also varies based on the inlet and exit temperatures of the drying chamber. At the initial phase of drying, the difference between the inlet and exit of the drying chamber is quite high in extracting moisture from the dried product due to the high moisture content of the drying sample in the beginning. Hence, at the beginning of the drying, the exergy efficiency of the dryer is low. Nonetheless, at the final stage of the drying, the moisture content of the drying sample is low. Accordingly, the discrepancy between the inlet and exit of the dryer is low, which causes higher exergy efficiency values to be acquired. A similar trend was encountered in the following studies investigating the exergy performance of varying types of drying chambers. In a vertical solar dryer they developed, Çiftçi et al. [37] reported the average exergy efficiency of the drying chamber between 41.85 and 52.01% in a system without fins. In the scenario with fins, these values varied between 43.04 and 56.11%, respectively. Sethi et al. [38] investigated the performances of solar dryers with absorber surfaces of V-grooved type and plate type. They observed that the exergy efficiency of the drying chamber of the V-grooved type system was higher at the rate of 3.47% than the plate-type system.

The primary purpose of a drying system is to reduce the product's water content as much as possible. From this aspect, the change in moisture content is another vital parameter in evaluating the performance of a drying system. The variation in the moisture content of the dried product in the designed systems is observed in Fig. 14. It is seen that better results were acquired during the drying process realized with the nano-enhanced solar dryer. At the end of the 360 min, the moisture ratio of the product in the nano-enhanced dryer declined to 0, while this value is 0.115 in the system, the absorber surface of which was covered with black matte paint. Depending on the obtained results, it can be said that the air temperature significantly affected the drying rate. In this context, significant improvements in drying time and drying rate can be achieved due to increasing the air exit temperature with different system modifications.

Furthermore, the airflow rate also causes significant changes in the drying rate. Çiftçi et al. [37] investigated the mint drying process on a vertical, finned solar dryer at different air flow rates. They obtained the drying time as 285, 240, and 195 min under 0.010, 0.012, and 0.014 kg/s flow rate conditions. Similarly, Khanlari et al. [39] investigated celery root drying with perforated and plus-shaped absorbent surfaces in a solar dryer. They found the drying time to be 225 min in the double-pass split system at a flow rate of 0.009 kg/s.

Figure 15 depicts the COP values of both designed solar drying systems. COP values change with temperature differences in the system. In addition, the airflow rate and the power consumed by the suction fans are among the parameters that affect the COP values. It is well known that the heating capacity and COP increase with any increment in environment temperature. In industrial applications, it is acknowledged that the COP value declines by 0.6–1.0 for every 10 °C temperature difference between the external unit and the exit

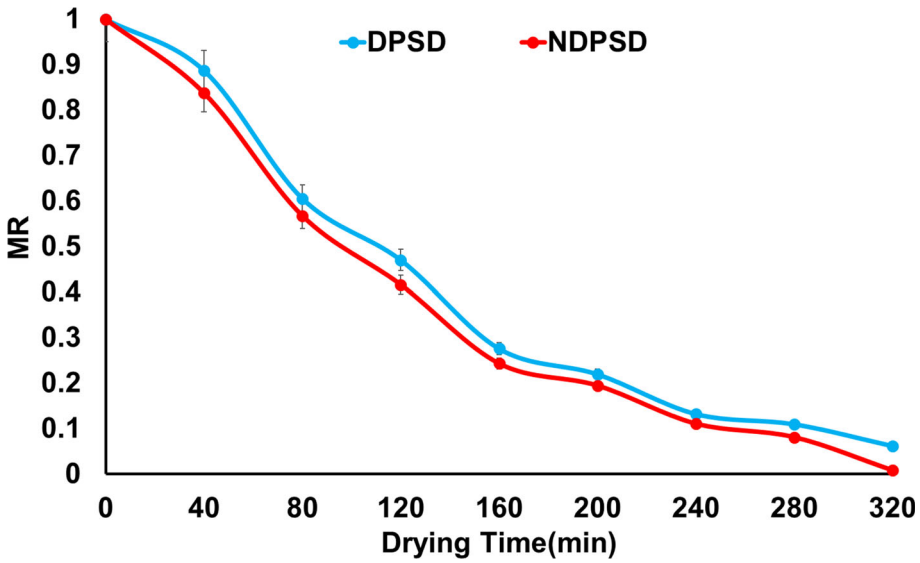


**Fig. 14** Variation in moisture ratio (MR) of the samples during the drying process

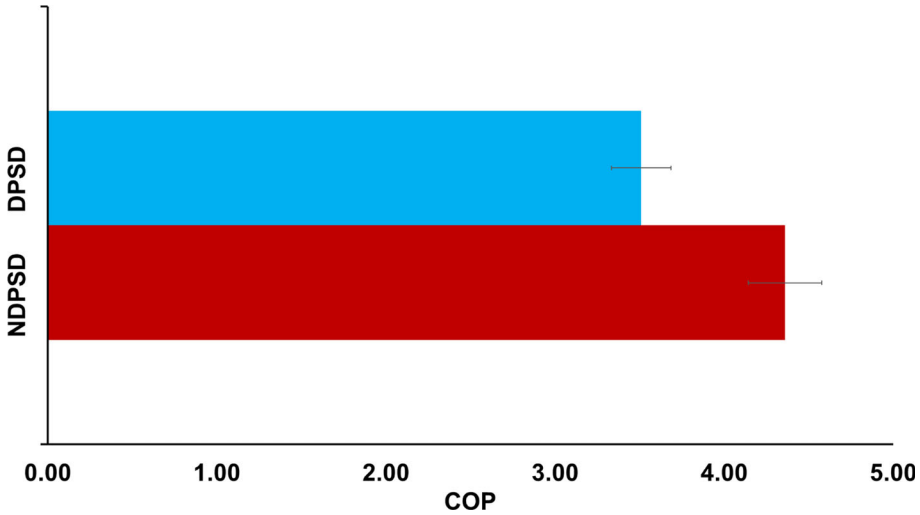


**Fig. 15** COP values of the solar collectors of each dryer

of the drying chamber. While the average COP value of the developed nano-enhanced solar dryer was 4.360, the COP value of the system covered with standard matte paint was calculated as 3.509. These values indicate an increase in the exit air temperature in the system with the nano-coating, which corresponds to an increase in COP as well. Similarly, Sözen et al. [6] performed a tube-type solar dryer performance analysis with iron mesh modification. They obtained the average COP value of the system with iron mesh modification between 3.10 and 3.35. Khanlari et al. [25] carried out experimental and numerical analyses on the solar air heater to upgrade the performance of the greenhouse dryer. They reported that the COP values of the system vary between 3.3 and 3.9 depending on the airflow rate.

The sustainability index of solar energy systems is one of the most fundamental parameters utilized for analyzing system performance and calculated by many researchers. The sustainability index values of both solar dryers are shown in Fig. 16. The average sustainability index of the solar dryers with a nano-enhanced absorber surface was obtained as 3.815. In contrast, the sustainability index of the solar dryers covered with black matte paint was calculated as 3.043. These values are anticipated to show a similar inclination with the exergy efficiency of the solar dryers. Therefore, as the moisture content of the product to be dried decreases, the sustainability index increases at the same rate. Furthermore, it can be said that the variation in air temperature also causes the sustainability index to fluctuate.

Another parameter examined for the assessment of the performance of solar dryers is the waste exergy ratio (WER). WER indicated the waste exergy is expected to show a contrasting characteristic with exergy and SI. In this sense, Fig. 17 shows the waste exergy ratio depending on the time of the drying chamber. The average WER value of the nano-enhanced solar dryer is 0.343, while the average WER value of the standard model is calculated as 0.409. As planned in

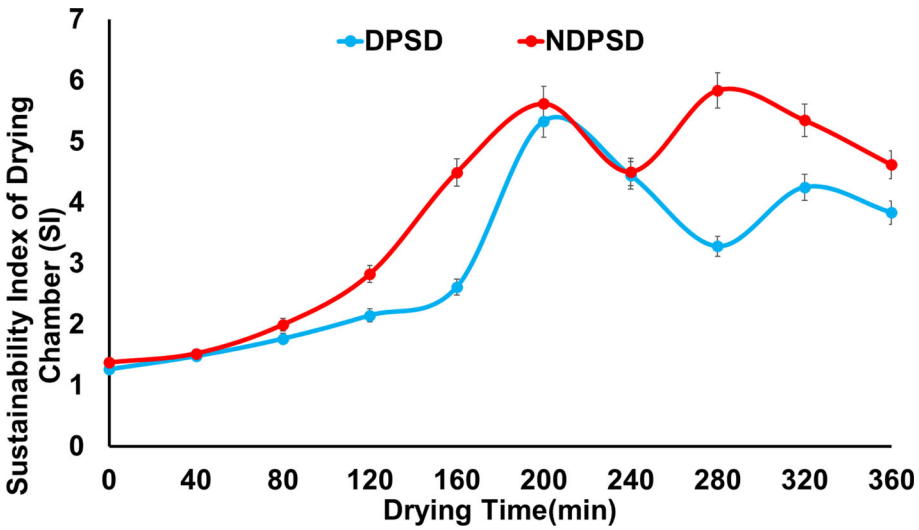


**Fig. 16** Variation in sustainability index (SI) values for drying chamber during the drying process

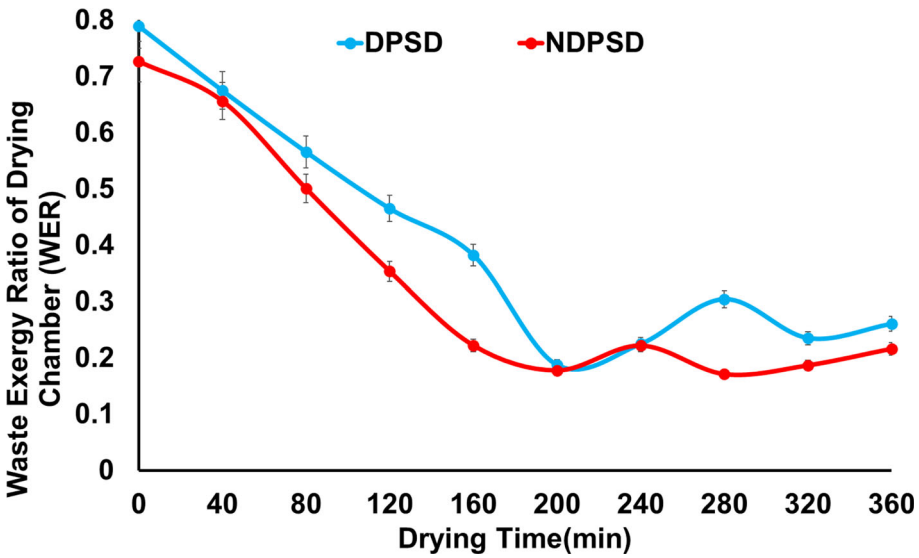


**Fig. 17** Variation in waste exergy ratio (WER) values for drying chamber during the drying process

line with the obtained values, the WER value is lower in the nano-enhanced model. The low exergy waste ratio indicates that the loss of exergy in the system is minimal.

Finally, Fig. 18 shows the electrical exergy changes of the photovoltaic panels integrated into the solar drying system. Based on the calculations, it was observed that the electrical exergy efficiencies for the designed systems varied between 0.944 and 1.904%. Considering that the photovoltaic panels used in the system were identical, the experiments were carried out simultaneously. In the same environmental conditions, it can be said that the calculated results are valid for both panels. In addition, the average electrical exergy value was calculated as 1.316. Table 4 illustrates the comparison of the present study with other state-of-the-art systems reported in the literature. Besides, the comparison of the costs of the solar dryers in the literature and the designed solar dryer is presented in Table 5. The economic analysis was made based on the annualized cost method [53, 54].

## 5 Conclusion

A new double-pass solar dryer was designed and experimentally analyzed in this work. The absorber surfaces were painted with graphene nanoparticles-doped black paint and standard black paint. The carrot slices were dried with hot air from the aluminum duct, which included a solar collector. Each system's general energy and exergy analyses used various performance parameters. Significant performance increments were observed due to modifying one of the systems with nanomaterials. The fundamental outcomes acquired from this study are as follows:

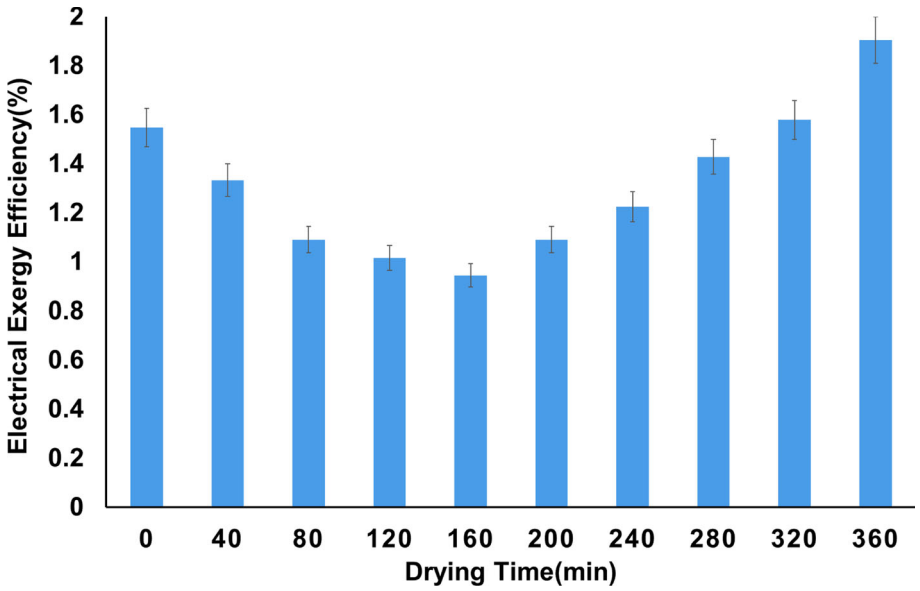


**Fig. 18** Variation in electrical exergy efficiency of PV panels

**Table 4** Comparison of the present study with state-of-the-art systems available in the literature

| Reference study | Collector type | Energy efficiency | Exergy efficiency |
|---|---|---|---|
| El-said et al. [40] | Vortex flow | 76.79% (0.050 kg/s, max.) | 1.30% (0.030 kg/s, max.) |
| Khanlari et al. [20] | Solar air heater with perforated baffles | 58.10–76.22% (nano-enhanced) | 13.10–14.46% (nano-enhanced) |
| Nazari et al. [15] | Flat plate with the serpentine tube (solar water heater) | - | 0.5–2.5% (CuO coated), 0.3–2% (black painted) |
| Selimefendigil et al. [17] | North wall with nanoparticles-included black paint | - | 5.38% (nano-enhanced) |
| Avargani et al. [41] | Vertical conical obstacles | 69.16% | 5.3% |
| Selimefendigil and Şirin [16] | Thermal energy storage | 75.02–50.13% (conventional), %52.43–78.08% (paraffin-based thermal energy storage), 57.73–82.19% (energy storage system coated with nano-material) | 10.52–13.59% (conventional), 11.08–14.36 (paraffin-based thermal energy storage), 12.52–15.44% (energy storage system coated with nano-material) |
| Muthukumaran and Senthil [42] | Thermal energy storage-integrated | 29.86% (0.0076 kg/s) | 1.11% (0.0076 kg/s) |
| Mgbemene et al. [43] | Single-pass and four-pass with waste aluminum soda cans | 15.2%-52.1% (single-pass), 39%-42.1% (four pass) | – |
| Moghadasi et al. [44] | Octagonal absorber surface | 78.73% | 32.87% |
| Selimefendigil et al. [19] | Solar air collector with triple-pass | 70.39–75.11% (nano-enhanced) | 9.05–10.18% (nano-enhanced) |
| Çiftçi et al. [37] | Vertical solar collector with sheet metal surfaces | 58.10–76.22% (nano-embedded) | 9.25–10.58% (nano-embedded) |
| Abdelkader et al. [21] | Solar heater with a flat plate | 50.65% (%4 CNTs/CuO), 40.71% (black painted) | 2.335% (%4 CNTs/CuO), 2.132% (black painted) |
| Akhbari et al. [45] | Triangular channel system with U-turn airflow pattern | %18.6-%33.4 | – |
| Tuncer et al. [46] | parallel pass, dual-pass, V-groove type | 54–60.29%, 61.86–66.95%, 70.91–78.18% (respectively) | 14.62–18.95%, 12.28–15.68%, 6.68–9.74% (respectively) |

**Table 4** (continued)

| Reference study | Collector type | Energy efficiency | Exergy efficiency |
|---|---|---|---|
| Abuşka [47] | Flat and conical surface | 74.6% (conical), 64.0% (flat) (0.1 kg/s) | 19.3% (conical), 16.1% (flat) (0.04 kg/s) |
| Kabeel et al. [48] | Baffled glazed bladed | 83.8% (0.04 kg/s) | – |
| Abdullah et al. [49] | Dual pass with turbulence | 68% (0.05 kg/s) | – |
| Abuşka and Şevik [50] | V-groove type | 43–60% | 6–12% |
| Benli ) [51] | Corrugated, trapezium, grooved reverse, inverted trapezium, base flat plate | 39%, 33%, 27%, 17%, 12% (respectively and 0.36 kg/s max.) | – |
| Gill et al. [27] | Low cost, dual, single glass, and packet bed | 30.29%, 45.05%, 71.68% | – |
| Present study | Double-pass solar collectors with and without nano-coating | 57.23% (without nano-coating), 73.36(with nano-coating) | 16.64% (without nano-coating), 27.77% (with nano-coating) |

**Table 5** Comparison of the costs of the present study to similar systems available in the literature

| Reference study | Costs ($) | Dryer type |
|---|---|---|
| Gilago et al. [52] | 1338/1873 | Indirect solar dryer/indirect solar dryer with *thermal energy storage system* |
| Philip et al. [53] | 2631 (material and labor charges) | 100 kg capacity greenhouse solar dryer |
| Kherrafi et al. [54] | 284.45/357.39 | Solar dryer with flat plate/solar dryer with offset strip fins |
| Madhankumar et al. [55] | 141.94/153.51/158.41 | Solar dryer without phase change material energy storage/solar dryer with phase change material energy storage/solar dryer with fins inserted phase change material energy storage |
| Heydari [56] | 347.91 | Hybrid dryer combined with spiral solar air heater and auxiliary heating system |
| Present work | 277.77 | Solar dryer system with double-pass absorber surfaces enhanced with graphene nanoparticles |

- While the average flow rates in the collectors of the designed solar drying systems were 0.017 kg/s for NDPSD, they were found to be 0.024 kg/s for DPSD. The average air flow rates in the drying chamber were measured as 0.012 and 0.016 kg/s for NDPSD and DPSD, respectively.
- The mean thermal efficiency of the collectors of the designed solar dryers was calculated as 73.36 and 57.23% for NDPSD and DPSD, respectively. Additionally, the average exergy efficiency of the solar collectors was estimated to be 27.77% for NDPSD and 16.64% for DPSD.
- Whereas the drying chamber exergy efficiency of solar dryers varied between 27.35 and 82.20% for NDPSD, this value altered between 21.03 and 81.25% for DPSD.
- The COP values of the solar air collectors in the system were obtained as 4.360 and 3.509 for NDPSD and DPSD, respectively.
- The sustainability index of drying chambers was calculated as 3.815 for NDPSD and 3.043 for DPSD.

Different material-based duct-type absorber plates can be used for photovoltaic–thermal solar collector systems with and without drying units for further studies. Some modifications, like mounting turbulators inside the tubes and extending the circulation time of the air in the collector by increasing the passing number (triple pass, etc.), can be tried for performance enhancement of such systems.

**Acknowledgements** This work was supported by Gazi University (Project No: FYL-2022-8194).

**Author's Contribution** MÖ involved in conceptualization, methodology, visualization, investigation, writing—reviewing and editing. CY took part in conceptualization, methodology, visualization, investigation, writing—reviewing and editing. EÇ involved in conceptualization, methodology, writing—reviewing and editing, supervision.

**Funding** Open access funding provided by the Scientific and Technological Research Council of Türkiye (TÜBİTAK).

## Declarations

**Conflict of interest** There is no conflict of interest in this study.

## References

1. Kong, D.; Wang, Y.; Li, M.; Liu, X.; Huang, M.; Li, X.: Analysis of drying kinetics, energy and microstructural properties of turnips using a solar drying system. Sol. Energy **230**, 721–731 (2021). https://doi.org/10.1016/j.solener.2021.10.073
2. Ortiz-Rodríguez, N.M.; Marín-Camacho, J.F.; Llamas-González, A.; García-Valladares, O.: Drying kinetics of natural rubber sheets under two solar thermal drying systems. Renew. Energy **165**, 438–454 (2021). https://doi.org/10.1016/j.renene.2020.11.035
3. Gürel, A.E.; Ağbulut, Ü.; Ergün, A.; Ceylan, İ; Sözen, A.; Tuncer, A.D.; Khanlari, A.: A detailed investigation of the temperature-controlled fluidized bed solar dryer: a numerical, experimental, and modeling study. Sustain. Energy Technol. Assess. **49**, 101703 (2022). https://doi.org/10.1016/j.seta.2021.101703
4. Afshari, F.; Khanlari, A.; Tuncer, A.D.; Sözen, A.; Şahinkesen, İ; Di Nicola, G.: Dehumidification of sewage sludge using quonset solar tunnel dryer: an experimental and numerical approach. Renew. Energy **171**, 784–798 (2021). https://doi.org/10.1016/j.renene.2021.02.158
5. Sözen, A.; Kazancıoğlu, F.Ş; Tuncer, A.D.; Khanlari, A.; Bilge, Y.C.; Gungor, A.: Thermal performance improvement of an indirect solar dryer with tube-type absorber packed with aluminum wool. Sol. Energy **217**, 328–341 (2021). https://doi.org/10.1016/j.solener.2021.02.029
6. Sözen, A.; Şirin, C.; Khanlari, A.; Tuncer, A.D.; Gürbüz, E.Y.: Thermal performance enhancement of tube-type alternative indirect solar dryer with iron mesh modification. Sol. Energy **207**, 1269–1281 (2020). https://doi.org/10.1016/j.solener.2020.07.072
7. Tuncer, A.D.; Sözen, A.; Khanlari, A.; Amini, A.; Şirin, C.: Thermal performance analysis of a quadruple-pass solar air collector assisted pilot-scale greenhouse dryer. Sol. Energy **203**, 304–316 (2020). https://doi.org/10.1016/j.solener.2020.04.030
8. Şevik, S.; Aktaş, M.; Dolgun, E.C.; Arslan, E.; Tuncer, A.D.: Performance analysis of solar and solar-infrared dryer of mint and apple slices using energy-exergy methodology. Sol. Energy **180**, 537–549 (2019). https://doi.org/10.1016/j.solener.2019.01.049
9. Krabch, H.; Tadili, R.; Idrissi, A.: Design, realization and comparison of three passive solar dryers. Orange drying application for the Rabat site (Morocco). Results Eng. **15**, 100532 (2022). https://doi.org/10.1016/j.rineng.2022.100532
10. Hassan, A.; Nikbahkt, A.M.; Welsh, Z.; Yarlagadda, P.; Fawzia, S.; Karim, A.: Experimental and thermodynamic analysis of solar air dryer equipped with V-groove double-pass collector: techno-economic and exergetic measures. Energy Convers. Manag.: X. **16**, 100296 (2022). https://doi.org/10.1016/j.ecmx.2022.100296
11. Veeramanipriya, E.; Sundari, A.U.: Performance evaluation of hybrid photovoltaic thermal (PVT) solar dryer for drying of cassava. Sol. Energy **215**, 240–251 (2021). https://doi.org/10.1016/j.solener.2020.12.027
12. Kale, S.G.; Havaldar, S.N.: Performance enhancement techniques for indirect mode solar dryer: a review. Mat. Today: Proc. **72**(3), 1117–1124 (2022). https://doi.org/10.1016/j.matpr.2022.09.177
13. Gilago, M.C.; Mugi, V.R.; Chandramohan, V.P.: Investigation of exergy-energy and environ-economic performance parameters of active indirect solar dryer for pineapple drying without and with energy storage unit. Sustain. Energy Technol. Assess. **53**, 102701 (2022). https://doi.org/10.1016/j.seta.2022.102701
14. Al-Kayiem, H.H.; Ismaeel, A.A.; Baheta, A.T.; Aurybi, M.A.: Performance enhancement of solar vortex power generator by Al2O3-in-black paint coating. J. Clean. Prod. **316**, 128303 (2021). https://doi.org/10.1016/j.jclepro.2021.128303
15. Nazari, M.; Jafarmadar, S.; Khalilarya, S.: Exergy and thermoeconomic analyses of serpentine tube flat-plate solar water heaters coated with CuO nanostructures. Case Stud. Therm. Eng. **35**, 102072 (2022). https://doi.org/10.1016/j.csite.2022.102072
16. Selimefendigil, F.; Şirin, C.: Energy and exergy analysis of a hybrid photovoltaic/thermal-air collector modified with nano-enhanced latent heat thermal energy storage unit. J. Energy Stor. **45**, 103467 (2022). https://doi.org/10.1016/j.est.2021.103467
17. Selimefendigil, F.; Şirin, C.; Öztop, H.F.: Improving the performance of an active greenhouse dryer by integrating a solar absorber north wall coated with graphene nanoplatelet-embedded black paint. Sol. Energy **231**, 140–148 (2022). https://doi.org/10.1016/j.solener.2021.10.082
18. Sivakumar, S.; Velmurugan, C.; Dhas, D.E.J.; Solomon, A.B.; Wins, K.L.D.: Effect of nano cupric oxide coating on the forced convection performance of a mixed-mode flat plate solar dryer. Renew. Energy **155**, 1165–1172 (2020). https://doi.org/10.1016/j.solener.2021.10.082
19. Selimefendigil, F.; Şirin, C.; Ghachem, K.; Kolsi, L.; Alqahtani, T.; Algarni, S.: Enhancing the performance of a greenhouse drying system by using triple-flow solar air collector with nano-enhanced absorber coating. Case Stud. Therm. Eng. **34**, 102011 (2022). https://doi.org/10.1016/j.csite.2022.102011
20. Khanlari, A.; Tuncer, A.D.; Sözen, A.; Aytaç, İ; Çiftçi, E.; Variyenli, H.İ: Energy and exergy analysis of a vertical solar air heater with nano-enhanced absorber coating and perforated baffles. Renew. Energy **187**, 586–602 (2022). https://doi.org/10.1016/j.renene.2022.01.074
21. Abdelkader, T.K.; Zhang, Y.; Gaballah, E.S.; Wang, S.; Wan, Q.; Fan, Q.: Energy and exergy analysis of a flat-plate solar air heater coated with carbon nanotubes and cupric oxide nanoparticles embedded in black paint. J. Clean. Prod. **250**, 11950 (2020). https://doi.org/10.1016/j.jclepro.2019.119501
22. Kabeel, A.E.; Sathyamurthy, R.; Sharshir, S.W.; Muthumanokar, A.; Panchal, H.; Prakash, N.; Prasad, C.; Nandakumar, S.; El Kady, M.S.: Effect of water depth on a novel absorber plate of pyramid solar still coated with TiO2 nano black paint. J. Clean. Prod. **213**, 185–191 (2019). https://doi.org/10.1016/j.jclepro.2018.12.185
23. Kumar, R.; Verma, S.K.; Sharma, V.K.: Performance enhancement analysis of triangular solar air heater coated with nanomaterial embedded in black paint. Mat. Today: Proc. **26**, 2528–2532 (2020). https://doi.org/10.1016/j.matpr.2020.02.538
24. Güler, H.Ö.; Sözen, A.; Tuncer, A.D.; Afshari, F.; Khanlari, A.; Şirin, C.; Gungor, A.: Experimental and CFD survey of indirect solar dryer modified with low-cost iron mesh. Sol. Energy **197**, 371–384 (2020). https://doi.org/10.1016/j.solener.2020.01.021
25. Khanlari, A.; Sözen, A.; Şirin, C.; Tuncer, A.D.; Gungor, A.: Performance enhancement of a greenhouse dryer: analysis of a cost-effective alternative solar air heater. J. Clean. Prod. **251**, 119672 (2020). https://doi.org/10.1016/j.jclepro.2019.119672
26. Krabch, H.; Tadili, R.; Bargach, M.: Indirect solar dryer with a single compartment for food drying. Application to the drying of the pear. Sol. Energy **240**, 131–139 (2022). https://doi.org/10.1016/j.solener.2022.05.025

27. Gill, R.S.; Singh, S.; Singh pp.: Low cost solar air heater. Energy Convers. Manag. **57**, 131–142 (2012). https://doi.org/10.1016/j.enconman.2011.12.019
28. Poole, M.R.; Shah, S.B.; Grimes, J.L.; Boyette, M.D.; Stikeleather, L.F.: Evaluation of a novel, low-cost plastic solar air heater for turkey brooding. Energy Sustain. Dev. **45**, 1–10 (2018). https://doi.org/10.1016/j.esd.2018.04.004
29. Ahmad, N.T.: Agricultural solar air collector made from low-cost plastic packing film. Renew. Energy **23**(3–4), 663–671 (2001). https://doi.org/10.1016/S0960-1481(00)00143-9
30. Ndukwu, M.C.; Onyenwigwe, D.; Abam, F.I.; Eke, A.B.; Dirioha, C.: Development of a low-cost wind-powered active solar dryer integrated with glycerol as thermal storage. Renew. Energy **154**, 553–568 (2020). https://doi.org/10.1016/j.renene.2020.03.016
31. Karabulut, K.; Buyruk, E.; Kılınç, F.: Grafen oksit nanoparçacıkları içeren nanoakışkanın taşınım ısı transferi ve basınç düşüşü artışı üzerindeki etkisinin düz bir boruda deneysel olarak araştırılması. Mühendis ve Makine. **59**(690), 45–67 (2018)
32. Çelik, A.N.: Analysis of Ankara's exposure to solar radiation: evaluation of distributional parameters using long-term hourly measured global solar radiation data. Turk. J. Eng. Environ. Sci. **30**(2), 115–126 (2006)
33. Holman, J.: Experimental methods for engineers, 7th edn. McGraw-Hill, New York (2001)
34. Khanlari, A.; Sözen, A.; Afshari, F.; Tuncer, A.D.: Energy-exergy and sustainability analysis of a PV-driven quadruple-flow solar drying system. Renew. Energy **175**, 1151–1166 (2021). https://doi.org/10.1016/j.renene.2021.05.062
35. Abbas, S.; Yuan, Y.; Hassan, A.; Zhou, J.; Ji, W.; Yu, T.; Ubal Ul, R.; Yousuf, S.: Design a low-cost, medium-scale, flat plate solar air heater: an experimental and simulation study. J. Energy Storage. **56**, 105858 (2022). https://doi.org/10.1016/j.est.2022.105858
36. Omojaro, A.P.; Aldabbagh, L.B.Y.: Experimental performance of single and double-pass solar air heater with fins and steel wire mesh as absorber. Appl. Energy **87**(12), 3759–3765 (2010). https://doi.org/10.1016/j.apenergy.2010.06.020
37. Çiftçi, E.; Khanlari, A.; Sözen, A.; Aytaç, İ; Tuncer, A.D.: Energy and exergy analysis of a photovoltaic thermal (PVT) system used in solar dryer: a numerical and experimental investigation. Renew. Energy **180**, 410–423 (2021). https://doi.org/10.1016/j.renene.2021.08.081
38. Sethi, C.K.; Acharya, S.K.; Ghanem, S.R.; Behera, A.; Patnaik, P.P.: Exergy, energy and economic analysis of a V-groove assist rotating tray type solar cabinet dryer for drying potato chips. J. Stored Prod. Res. **93**, 101861 (2021). https://doi.org/10.1016/j.jspr.2021.101861
39. Khanlari, A.; Güler, H.Ö.; Tuncer, A.D.; Şirin, C.; Bilge, Y.C.; Yılmaz, Y.; Güngör, A.: Experimental and numerical study of the effect of integrating plus-shaped perforated baffles to solar air collector in drying application. Renew. Energy **145**, 1677–1692 (2020). https://doi.org/10.1016/j.renene.2019.07.076
40. El-Said, E.M.; Abou Al-Sood, M.M.; Elsharkawy, E.A.; Abdelaziz, G.B.: Tubular solar air heater using finned semi-cylindrical absorber plate with swirl flow: experimental investigation. Sol. Energy **236**, 879–897 (2022). https://doi.org/10.1016/j.solener.2022.03.054
41. Avargani, V.M.; Zendehboudi, S.; Rahimi, A.; Soltani, S.: Comprehensive energy, exergy, enviro-exergy, and thermo-hydraulic performance assessment of a flat plate solar air heater with different obstacles. Appl. Therm. Eng. **203**, 117907 (2022). https://doi.org/10.1016/j.applthermaleng.2021.117907
42. Muthukumaran, J.; Senthil, R.: Experimental performance of a solar air heater using straight and spiral absorber tubes with thermal energy storage. J. Energy Stor. **45**, 103796 (2022). https://doi.org/10.1016/j.est.2021.103796
43. Mgbemene, C.; Jacobs, I.; Okoani, A.; Ononiwu, N.: Experimental investigation on the performance of aluminum soda can solar air heater. Ren. Energy. **195**, 182–193 (2022). https://doi.org/10.1016/j.renene.2022.06.011
44. Moghadasi, M.; Ghadamian, H.; Khodsiani, M.; Pourbafrani, M.: A comprehensive experimental investigation and dynamic energy modeling of a highly efficient solar air heater with octagonal geometry. Sol. Energy **242**, 298–311 (2022). https://doi.org/10.1016/j.solener.2022.07.030
45. Akhbari, M.; Rahimi, A.; Hatamipour, M.S.: Modeling and experimental study of a triangular channel solar air heater. Appl. Therm. Eng. **170**, 114902 (2020). https://doi.org/10.1016/j.applthermaleng.2020.114902
46. Tuncer, A.D.; Khanlari, A.; Sözen, A.; Gürbüz, E.Y.; Şirin, C.; Gungor, A.: Energy-exergy and enviro-economic survey of solar air heaters with various air channel modifications. Renew. Energy **160**, 67–85 (2020). https://doi.org/10.1016/j.renene.2020.06.087
47. Abuşka, M.: Energy and exergy analysis of solar air heater having new design absorber plate with conical surface. Appl. Therm. Eng. **131**, 115–124 (2018). https://doi.org/10.1016/j.applthermaleng.2017.11.129
48. Kabeel, A.E.; Hamed, M.H.; Omara, Z.M.; Kandel, A.W.: On the performance of a baffled glazed-bladed entrance solar air heater. Appl. Therm. Eng. **139**, 367–375 (2018). https://doi.org/10.1016/j.applthermaleng.2018.04.141
49. Abdullah, A.S.; Abou Al-Sood, M.M.; Omara, Z.M.; Bek, M.A.; Kabeel, A.E.: Performance evaluation of a new counter flow double pass solar air heater with turbulators. Sol. Energy **173**, 398–406 (2018). https://doi.org/10.1016/j.solener.2018.07.073
50. Abuşka, M.; Şevik, S.: Energy, exergy, economic and environmental (4E) analyses of flat-plate and V-groove solar air collectors based on aluminum and copper. Sol. Energy **158**, 259–277 (2017). https://doi.org/10.1016/j.solener.2017.09.045
51. Benli, H.: Experimentally derived efficiency and exergy analysis of a new solar air heater having different surface shapes. Renew. Energy **50**, 58–67 (2013). https://doi.org/10.1016/j.renene.2012.06.022
52. Gilago, M.C.; Mugi, V.R.; Chandramohan, V.P.: Energy-exergy and environ-economic (4E) analysis while drying ivy gourd in a passive indirect solar dryer without and with energy storage system and results comparison. Sol. Energy **240**, 69–83 (2022). https://doi.org/10.1016/j.solener.2022.05.027
53. Philip, N.; Duraipandi, S.; Sreekumar, A.: Techno-economic analysis of greenhouse solar dryer for drying agricultural produce. Renew. Energy **199**, 613–627 (2022). https://doi.org/10.1016/j.renene.2022.08.148
54. Kherrafi, M.A.; Benseddik, A.; Saim, R.; Bouregueba, A.; Badji, A.; Nettari, C.; Bensaha, H.: Performance enhancement of indirect solar dryer with offset strip fins: experimental investigation and comparative analysis. Sol. Energy **266**, 112158 (2023). https://doi.org/10.1016/j.solener.2023.112158
55. Madhankumar, S.; Viswanathan, K.; Wu, W.; Taipabu, M.I.: Analysis of indirect solar dryer with PCM energy storage material: energy, economic, drying and optimization. Sol. Energy **249**, 667–683 (2023). https://doi.org/10.1016/j.solener.2022.12.009
56. Heydari, A.: Experimental analysis of hybrid dryer combined with spiral solar air heater and auxiliary heating system: energy, exergy and economic analysis. Renew. Energy **198**, 1162–1175 (2022). https://doi.org/10.1016/j.renene.2022.08.110